Testing the Response of Several Dosimeters to X-Ray Radiation

Luka Lotina*, Paula Antonija Bačani, Gabriela Jazvac, Ana Marija Kožuljević, Luka Pavelić**
Institute for Medical Research and Occupational Health, Division of Radiation Protection
Ksaverska cesta 2, 10000 Zagreb, Croatia
*llotina@imi.hr, **lpavelic@imi.hr

ABSTRACT

When working with radioactive sources in hospitals, nuclear power plants or research facilities, in order to prevent individuals from being overexposed to radiation, a precise measurement of radiation is of crucial importance. For this reason, there are a number of available dosimeters which are regularly used in those facilities. Since these devices can differ in precision and in the way they detect radiation, it is useful to compare the responses of different dosimeters when exposed to radiation beams. In this paper, we present the results we obtained by testing the responses of several commercially available dosimeters to different beams of X-ray radiation. For each dosimeter, we performed two measurements. Firstly, we irradiated the 1 L spherical ionization chamber, located at the distance of 2 meters from the radioactive source, with beams N-25, N-30, N-40, N-60, N-80, N-100, N-120, N-150 and N-200, with the current being kept at 10 mA. For each beam, the ionization chamber was irradiated until the measured H*(10) dose was approximately 1 mSv. After that, the dosimeters were set at the same distance from the source as the ionization chamber and irradiated with the same beams and for the same amount of time as the chamber. In the second set of measurements, we measured the dependence of the dosimeter response on the dose rate. For this set, the ionization chamber was irradiated by the RQR-8 beam at 100 kV tube potential, while the current was varied, so that the dose rate would change. For each current, the chamber was irradiated until the measured H*(10) dose was again approximately 1 mSv. The dosimeters were then irradiated for the same set of currents and for the same amount of time for each current value. For each dosimeter, the results of the first set of measurements were normalized with respect to the response obtained for the N-100 beam and plotted as a function of the tube potential. For the second set of measurements, the responses of dosimeters were plotted as a function of dose rates.

Keywords: *dosimeters, ionization chamber, X-ray beams, H*(10), dose rate*

1 INTRODUCTION

Radiation safety is one of the most important aspects when working in fields where exposure is expected, e.g. nuclear energy, radiodiagnostics and radiotherapy in hospitals, research in experimental nuclear physics etc. A general safety guide is given by the International Atomic Energy Agency (IAEA) [1], and, in the European Union, there are regulations that proscribe the radiation monitoring of different categories of radiation workers [2]. The International Commission on Radiation Protection (ICRP) recommends the quantity called the ambient dose equivalent $H^*(10)$, as an operational quantity to assess the effective dose in area monitoring [3, 4].

To measure the $H^*(10)$ doses, various dosimeters can be used, that are typically divided into 2 categories: active dosimeters (ADs) [5, 6] and passive dosimeters (PDs) [7]. The main difference between the two categories is that ADs are able to also provide an in-real-time measurement of the ambient equivalent dose rate $H^*(10)/t$, while PDs can only measure the total accumulated $H^*(10)$ dose. The most common types of detectors used by the ADs are the ionization chamber, the

proportional counter and the Geiger-Müller (GM) tube [8], while the most common PDs are the thermoluminescent dosimeters (TLDs) and optically stimulated luminescent dosimeters (OSLDs) [9]. Due to the fact that dosimeters use different types of radiation detection mechanisms, it is expected that their responses to different types of radiation will differ from one another. Because of this, dosimeter responses need to be tested on various types of radiation, and the inter-comparisons of dosimeter responses to different types of radiological beams are regularly performed in laboratories all over the world [10, 11, 12]. In this paper, we present the results we obtained by testing the responses of 5 different commercially available dosimeters at the Institute for Medical Research and Occupational Health (IMI) to narrow protection beams (N-series) [13], defined by the International Organization for Standardization (ISO). We also studied how the response of each dosimeter depends on the $H^*(10)/t$ dose rate of the diagnostic beam of the RQR-series [14], defined by the International Electrotechnical Commission (IEC). The obtained results were compared to the existing experimental data and the available data from the dosimeter manufacturers' instructions manuals.

2 EXPERIMENTAL SETUP AND METHODS

The experiment was carried out at the IMI's Metrology X-ray irradiation laboratory, using a modern X-ray generator, capable of producing various types of radiological beams [15]. The chosen N-series beams were N-25, N-30, N-40, N-60, N-80, N-100, N-120, N-150 and N-200, with each number in the name corresponding to the voltage $U(\mathrm{kV})$ set on the X-ray generator tube. The chosen beam of the RQR-series was RQR-8, corresponding to $U = 100\ \mathrm{kV}$. The RQR-8 beam was chosen due to a large range of dose rates that can be generated with that beam. For a reference chamber, a 1L spherical ionization chamber from PTW was chosen [16]. This chamber was calibrated on N-40, N-60, N-80, N-100, N-150 and N-200 beams.

2.1 Dosimeters

The selected dosimeters were ADs Thermo FH 40G-L10 [17], Thermo FHZ 312A [18], Mirion SPIR-Ace [19], STEP OD-02 [20] and a passive Mirion Area BeOSL dosimeter (BeOSLD) [21]. The specifications for each dosimeter, including the manufacturer, the detector type and the minimum and maximum dose rates that can be measured by each dosimeter are given in Table 1.

Table 1: Specifications of studied dosimeters

Dosimeter	Manufacturer	Detector type	Min. dose rate (μSv/h)	Max. dose rate (mSv/h)
Thermo FH 40G-L10	Thermo Fisher Scientific	Proportional counter	0.01	100
Thermo FHZ 312A	Thermo Fisher Scientific	Proportional counter	10	10000
Mirion SPIR-Ace	Mirion Technologies	GM tube	100	100
STEP OD-02	STEP	Ionization chamber	20	2000
Mirion Area BeOSL	Mirion Technologies	BeO OSLD	no limit	no limit

It is important to mention that the SPIR-Ace dosimeter consists of two detectors; the $LaBr_3$ scintillation detector, capable of identifying the type of radiation, and a GM tube [19], however, due to the fact that the $LaBr_3$ detector can only measure radiations with dose rates up to $100\ \mu\mathrm{Sv/h}$, this detector was not suitable for testing at the X-ray generator, which is not able to produce stable radiological beams with dose rates less than $\sim 1\ \mathrm{mSv/h}$.

2.2 Measuring the relative response of dosimeters to beams of different photon energies

The study of the dependence of dosimeter responses to beams of different nominal photon energies was performed by measuring the relative dosimeter responses to beams of the N-series, listed above. Each beam corresponds to a particular nominal photon energy, which can be found in Ref. [13]. The experiment was carried out in the following way; firstly, a reference chamber was fixed at a distance $d_C = 2$ m from the radiation source, and positioned in a way so that the incident angle of the radiation beam is $\alpha = 0°$. The current on the cathode of the X-ray generator was set to 10 mA. For each N-series beam, the chamber was irradiated until the accumulated dose was measured to be ~1 mSv. After each irradiation, the values that were recorded were: $H^*(10)_C$ dose, the irradiation time t_C, temperature T_C and pressure p_C of the room and the monitor chamber, and the accumulated charge on the monitor chamber M_C, measured by the electrometer in the control room.

After the irradiation of the reference chamber was completed, each dosimeter was positioned at a distance $d_D = d_C = 2$ m from the source, and fixed, so that $\alpha = 0°$. Each dosimeter was then irradiated with each of the N-series beams for the same time $t_D = t_C$. The recorded values for each irradiation were: $H^*(10)_D$ dose measured by the dosimeter, irradiation time t_D, temperature T_D and pressure p_D and the charge M_D accumulated on the monitor chamber during the irradiation of the dosimeter. In the case of Area BeOSLDs, for each irradiation, 3 separate BeOSLDs were positioned next to each other, and irradiated together. The chosen beams for BeOSLDs were: N-25, N-40, N-60, N-80, N-100, N-150 and N-200.

2.3 Measuring the dependence of relative dosimeter responses on varying dose rates

The dependence of the relative response on $H^*(10)/t$ dose rates was tested on the RQR-8 beam. The voltage was set to $U = 100$ kV, and the current I on the cathode of the X-ray generator was varied in order to achieve different average dose rate values. The values of I and the average dose rates measured on the reference chamber are shown in Table 2.

Table 2: Currents on the X-ray generator and corresponding dose rates measured by the reference chamber

I(mA)	Approximate average $H^*(10)_C/t_C$ (mSv/h)
0.3	30
0.4	40
0.5	60
0.6	70
0.7	85
0.9	100
1.1	125
1.4	155
2.2	315
3.6	500

This part of the experiment was carried out similarly to the first part. Firstly, the reference chamber was positioned so that $d_C = 2$ m and $\alpha = 0°$. The chamber was then irradiated for each value of I and the same values were recorded as in the first part of the experiment.

After the irradiation of the reference chamber was completed, each dosimeter was irradiated in the same way as in the first part of the experiment, with the same values being recorded. In the case of BeOSLDs, each measurement was performed on 3 BeOSLDs simultaneously, and the chosen currents for BeOSLDs were 0.3 mA, 0.4 mA, 0.6 mA, 0.7 mA, 1.4 mA, 2.2 mA and 3.6 mA.

2.4 Calculating the relative response and estimating the uncertainty budget

The relative dosimeter response is given by the relation:

$$R_D = \frac{H^*(10)_D}{H^*(10)_C \cdot k_{pT_C} \cdot k(Q, 0°)} \cdot \frac{M_C \cdot k_{pT_C}}{M_D \cdot k_{pT_D}} \cdot \frac{t_C}{t_D} \cdot \frac{d_D^2}{d_C^2}, \quad (1)$$

where

$$k_{pT_i} = \frac{p_0 \cdot T_i}{p_i \cdot T_0}, \; i = C, D \quad (2)$$

is the correction factor for temperature and pressure, that were measured during the irradiation of the reference chamber or a dosimeter, with $T_0 = 20℃ = 293.15$ K and $p_0 = 1013.25$ hPa representing the reference temperature and pressure values. In the case of the STEP OD-02 dosimeter, the instruction manual states that a measured $H^*(10)_D$ dose should also be multiplied by a correction factor k_{pT_D} [20]. The $k(Q, 0°)$ factor is called the quality factor of the reference chamber for an incident irradiation angle $\alpha = 0°$, and is obtained by calibrating the reference chamber on a particular radiological beam. The values of $k(Q, 0°)$ are shown in Table 3.

Table 3: Values of the quality factor $k(Q, 0°)$ for the reference chamber

Beam	$k(Q, 0°)$
N-25	0.468
N-30	0.561
N-40	0.746
N-60	0.934
N-80	1.007
N-100	1.000
N-120	0.975
N-150	0.931
N-200	0.862
RQR-8	1.000

In the case of the 1L PTW spherical chamber, $k(Q, 0°)$ was determined for beams N-40, N-60, N-80, N-100, N-150 and N-200. For N-25 and N-30 beams, we obtained the $k(Q, 0°)$ from extrapolation, and, in the case of the N-120 beam, from interpolation. Both the interpolation and the extrapolation were performed using a cubic spline method [22]. Since the reference chamber was not calibrated on any beam of the RQR-series, the factor was assumed to be $k(Q, 0°) = 1.0$ for the RQR-8 beam, because the goal of that part of the experiment was to study how the measured relative response changes when the dose rate is varied, rather than to precisely measure the relative response.

What can be noticed in Eq. (1) is that the two k_{pT_C} factors cancel each other out, and also, factors $\frac{t_C}{t_D} = \frac{d_D^2}{d_D^2} = 1$ do not contribute to the resulting relative response R_D. For the STEP OD-02 dosimeter, factors k_{pT_D} also cancel each other out. While these factors do not contribute to the value of R_D, their uncertainties contribute to the total uncertainty of the relative response $u(R_D)$, and for that reason, they are included in Eq. (1).

The uncertainty budget is estimated in the following way; firstly, for some dosimeters, e.g. STEP OD-02, the instructions manual gives an uncertainty error of the measured $H^*(10)_D$ dose [20]. Secondly, the uncertainties and distribution types of temperature T, pressure p and the accumulated charge M were obtained from the calibration certificates of measuring devices, while the uncertainties

of the quality factor $k(Q,\ 0°)$ were obtained from the calibration certificate of the reference chamber. The uncertainties of the measured time and distance were estimated to be $u(t) = 0.1$ s and $u(d) = 0.1$ cm, and the B-type rectangular distribution was assumed for those uncertainties following the Guide to the expression of uncertainty in measurement (GUM) [23] and the recommendations relating to estimating the uncertainties in dosimetry [24]. Finally, in the case of BeOSLDs, an additional A-type uncertainty was present due to the fact that the measured $H^*(10)_D$ dose for every beam was taken to be the arithmetic mean of the doses measured by each of the 3 dosimeters. The calculation of doses and the estimation of the uncertainty budget was done using the Python GUM tree calculator (GTC) package [25].

3 RESULTS

3.1 Relative responses of dosimeters to beams of different photon energies

The budget uncertainty calculation was performed only for beams on which the reference chamber was calibrated. The graphs of relative responses of selected dosimeters, plotted as a function of the X-ray tube voltage, are shown in Fig. 1.

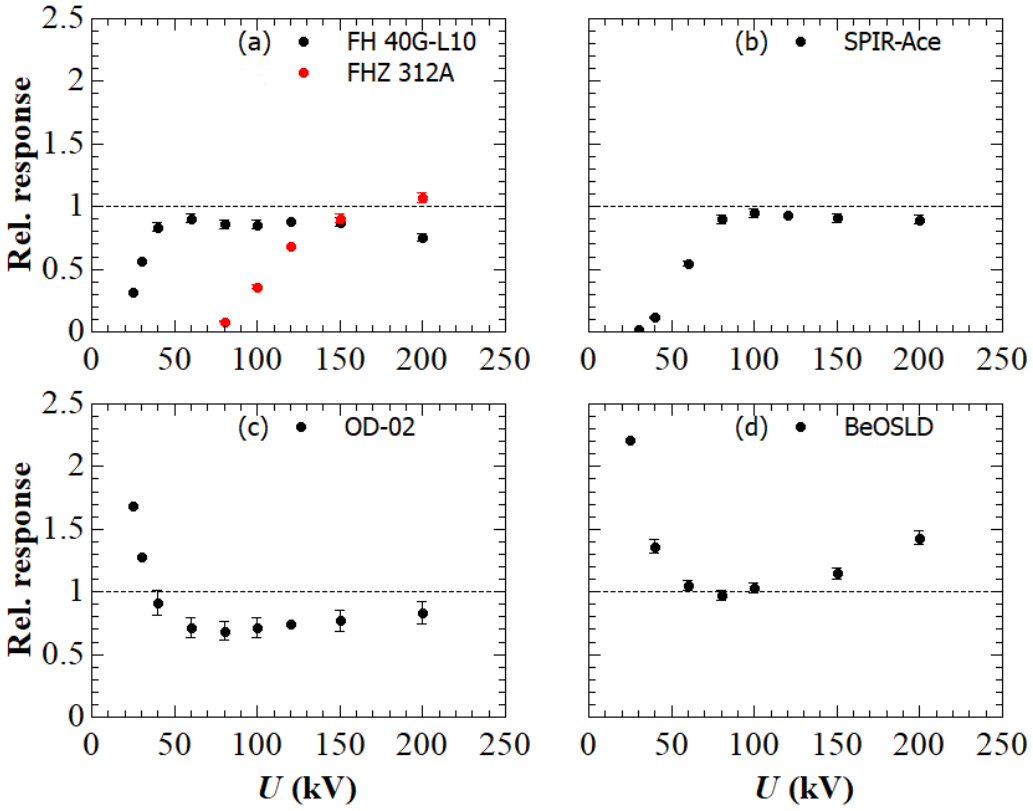

Figure 1: Relative responses of: (a) Thermo FH 40G-L10 and Thermo FHZ 312A, (b) SPIR-Ace, (c) STEP OD-02 and (d) Area BeOSLD. The dotted line represents the relative response $R_D = 1.0$.

Fig. 1(a) shows the relative responses of Thermo FH 40G-L10 and Thermo FHZ 312A dosimeters. The FH 40G-L10 has a satisfying response for beams of N-40 and above, while for beams of lower nominal photon energy, i.e. N-25 and N-30, it is not able to properly detect low-energy photons. The FHZ 312A, on the other hand, shows a significant insensitivity to photons below $E_\gamma = 100$ keV (N-120 beam). This can be explained by the fact that the stainless-steel coat, that covers the surface of the dosimeter, can block low energy photons before they reach the proportional counter

detector inside. A similar behaviour to FH 40G-L10 can also be observed for the SPIR-Ace dosimeter (Fig. 1(b)). This dosimeter has a satisfying relative response for beams N-80 and above, while not being able to properly detect beams of lower nominal photon energies. A potential explanation for this behaviour is that the walls of the proportional counter of FH 40G-L10 and of the GM tube of SPIR-Ace block photons of lower energies before they are able to reach the detectors. The STEP OD-02 (Fig. 1(c)) and Area BeOSLD (Fig. 1(d)), on the other hand, show a different behaviour of relative responses. The OD-02 dosimeter is very sensitive to low-energy radiation, while for beams N-60 and above, it shows a relatively stable response with values slightly increasing from $R_D \approx 0.7$ for the N-60 beam to $R_D \approx 0.8$ for the N-200 beam. The BeOSLD shows an even stronger sensitivity to low-energy beams, with a response of $R_D \approx 2.3$ for the N-25 beam. The response decreases to $R_D \approx 0.95$ for the N-80 beam, and then increases again to $R_D \approx 1.45$ for the N-200 beam.

Since the dosimeter responses are typically presented normalized to the response for a particular radiological beam, we are showing the relative responses of selected dosimeters normalized to their responses at N-100, and compared to the results that can be found in the instructions manuals. That data is available for all of the dosimeters, except for the SPIR-Ace. In Fig. 2 we show the normalized relative dosimeter responses compared to the data from instructions manuals.

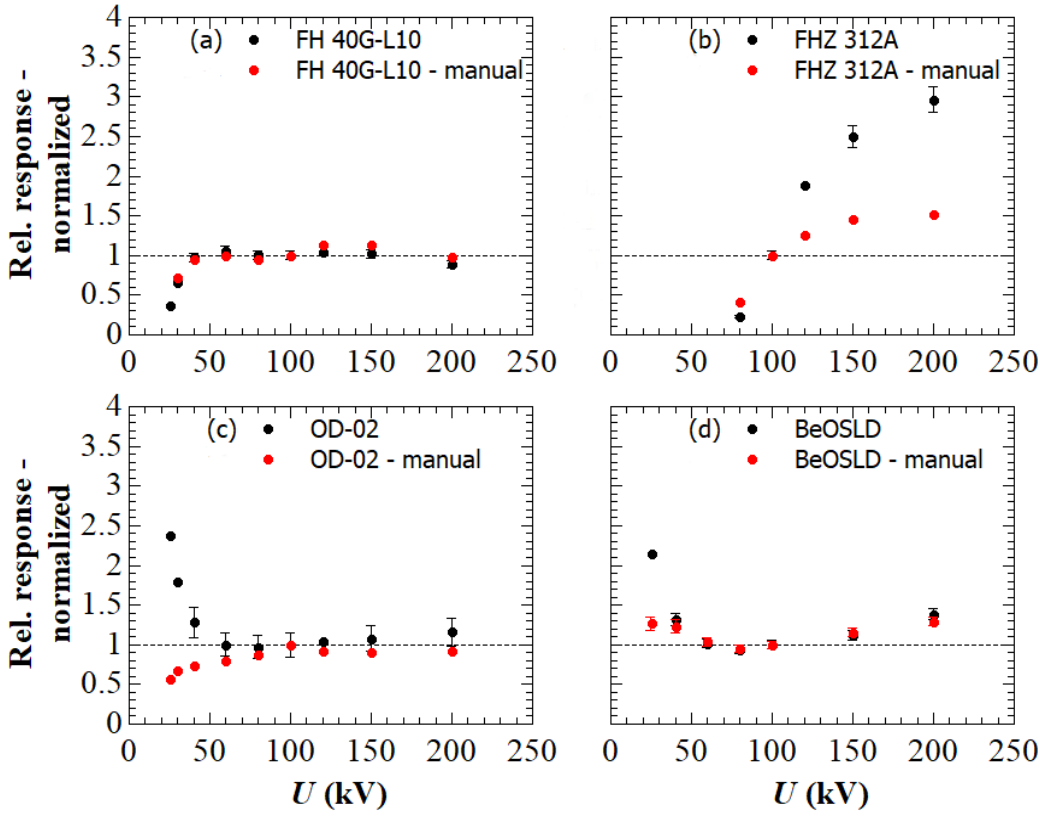

Figure 2: Relative responses of dosimeters, normalized to the response for the N-100 beam, plotted as a function of the X-ray tube voltage and compared to the available data from instruction manuals: (a) Thermo FH 40G-L10, (b) Thermo FHZ 312A, (c) STEP OD-02 and (d) Area BeOSLD. The data for (b), (c) and (d) can be found in Refs. [18, 20, 21], respectively.

Fig. 2(a) shows the normalized response of the FH 40G-L10, which is in good agreement with the data from the instruction manual. On the other hand, it can be seen from Fig. 2(b) that our experiment shows a significantly more sensitive response of the FHZ 312A dosimeter to beams above N-100, compared to the instructions manual results. The results for the OD-02 from Fig. 2(c) show a good agreement with the data from the manual, with the exception of beams N-40 and below, for which our experiment predicts a significantly more sensitive response. Our measurements of the

responses of the BeOSLD (Fig. 2(d)) are also in good agreement with the manual data, the exception being the response for the N-25 beam. The disagreement between our and manufacturers' measurement results in Figs. 2(c) and (d) could potentially be explained by the fact that for N-25 and N-30 beams, the factor $k(Q,\ 0°)$ was obtained by the extrapolation method, which is not always reliable. However, that still cannot explain the differences for the N-40 beam in Fig. 2(c). Since the experimental method for obtaining the results in the instructions manual is not known, we cannot be certain where those differences arise from.

3.2 Dependence of dosimeter responses on varying dose rates

The graphs of relative dosimeter responses, plotted as a function of the measured dose rates on the reference chamber, are shown in Fig. 3.

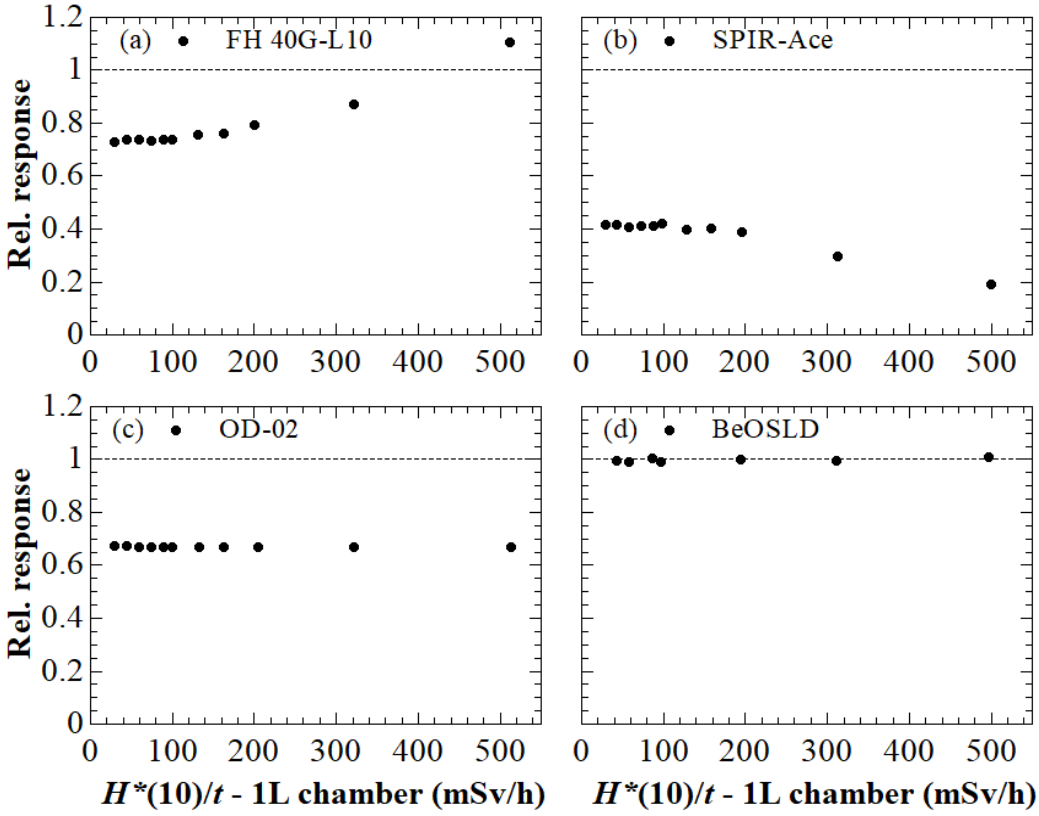

Figure 3: Relative response of dosimeters as a function of the measured dose rate on the reference chamber: (a) Thermo FH 40G-L10, (b) SPIR-Ace, (c) STEP OD-02 and (d) Area BeOSLD.

Fig. 3(a) shows the response of the FH 40G-L10 dosimeter, which seems to increase after the measured dose rate on the dosimeter crosses the 100 mSv/h threshold. This is not expected for a dosimeter with a proportional counter detector, which implies that there are compensation factors included in the detection system, with which the measured $H^*(10)_D$ dose is multiplied after the aforementioned threshold is crossed. This kind of behaviour for FH 40G-L10 was also observed in a different experiment [12]. The GM detector of SPIR-Ace in Fig. 3(b), on the other hand shows the opposite behaviour, with the response sensitivity decreasing after the detector threshold is crossed. This kind of behaviour is expected for the GM tube, primarily due to the time between different ionizing events being shorter than the dead time of the detector [8]. The OD-02 and the BeOSLD from Figs. 3(c) and (d), respectively, show no dependence of the relative response on the varying dose rate. The FHZ 312A dosimeter response is not shown due to the fact that this dosimeter is not sensitive to photons of the RQR-8 beam.

4 CONCLUSION

The selected dosimeters show a good relative response to different beams of photon energies. The dosimeters using a proportional counter or a GM tube are not sensitive to low-energy photons, with the FHZ 312A device being unable to properly detect photons below approximately 100 keV. On the other hand, the ionization chamber dosimeter STEP OD-02 and the Area BeOSLD show a good response for all of the selected radiological beams. The proportional counter FH 40G-L10 and the GM tube SPIR-Ace dosimeters show a change in the measured responses after a 100 mSv/h threshold is crossed, with the former's response increasing, and the latter's response decreasing. The responses of OD-02 and BeOSLD show no dependence on the varying dose rate.

A planned continuation of this research is the measurement of the dependence of the dosimeter responses on the incident angle of radiation beams. This will be performed on all of the selected dosimeters for all of the beams the reference chamber was calibrated on. Furthermore, the reference chamber could be calibrated on the N-25 and N-30 beams, as well as on the diagnostic beams of the RQR-series, in order to properly measure the relative responses.

ACKNOWLEDGEMENTS

This research was funded by the European Union – Next Generation EU and is part of the project Voxel Matrix Detector for Full Solid Angle Radiological Imaging – VMDScan - NPOO.C3.2.R2-I1.06.0084.

REFERENCES

[1] International Atomic Energy Agency, IAEA, Occupational radiation protection - General safety guide no. GSG-7 (2018)

[2] Euratom, Council directive 2013/59/Euratom of 5 December 2013. Laying Down basic safety standards for protection against the dangers arising from exposure to ionizing radiation, *Official Journal of the European Union L*, 13 (2013), pp. 1-73

[3] International Commission on Radiological Protection, The 2007 Recommendations of the International Commission on Radiological Protection. *ICRP Publication* 103, 2007.

[4] R. Casanovas, E. Prieto, M. Salvadó, Calculation of the ambient dose equivalent H*(10) from gamma-ray spectra obtained with scintillation detectors, *Applied Radiation and Isotopes*, Vol. 118, pp. 154-159, 2016.

[5] U. O'Connor, E. Carinou, I. Clairand, O. Ciraj-Bjelac, F. De Monte, J. Domienik-Andrzejewska, P. Ferrari, M. Ginjaume, H. Hršak, O. Hupe, Ž. Knežević, M. Sans Merce, S. Sarmento, T. Siiskonen, F. Vanhavere, Recommendations for the use of active personal dosimeters (APDs) in interventional workplaces in hospitals, *Physica Medica*, Vol. 87, pp. 131-135, 2021.

[6] F. Vanhavere, O. Van Hoey, Advances in personal dosimetry towards real-time dosimetry, *Radiation Measurements*, Vol. 158, 2022.

[7] Z. Yang, H. Vrielinck, L. G. Jacobsohn, P. F. Smet, D. Poelman, Passive Dosimeters for Radiation Dosimetry: Materials, Mechanisms, and Applications, *Advanced Functional Materials*, Vol. 34, 2024.

[8] S. R. Cherry, J. A. Sorenson, M-. E. Phelps, Physics in Nuclear Medicine, 4th ed. Saunders Elsevier, Philadelphia, 2012.

[9] J. Stanković Petrović, Ž. Knežević, N. Kržanović, M. Majer, M. Živanović, O. Ciraj-Bjelac, Review of the thermoluminescent dosimetry method for the environmental dose monitoring, *Nuclear Technology & Radiation Protection*, Vol. 36 (2), pp. 150-162, 2021.

[10] L. Oliver, C. Candela-Juan, J.D. Palma, M.C. Pujades, A. Soriano, J. Vilar, J.M. Martínez, V. Mestre, J.C. Ruiz-Rodríguez, N. Llorca-Domaica, Comparison of the dosimetric response of 4-elements OSL and TL passive personal dosimeters, *Radiation Measurements*, Vol. 107, pp. 128-135, 2017.

[11] G. Zorloni, I. Ambrožová, P. Carbonez, M. Caresana, S. Ebert, V. Olšovcová, A. Pitzschke, O. Ploc, F. Pozzi, M. Silari, F. Trompier, R. Trunecek, Z. Zelenka, Intercomparison of personal and ambient dosimeters in extremely high-dose-rate pulsed photon fields, *Radiation Physics and Chemistry*, Vol. 172, 2020.

[12] J. Vlahović, N. Kržanović, M. Živanović, I. Stojanović, L. Bakrač, A. Boziari, M. Đaletić, A. Fernandes, L.-C. Mihailescu, E. Reyhanoglu, S. Saroka, T. Siiskonen, J. Šmoldasová, V. Sochor, M. do Ceu Ferreira, N. Todorović, Performance assessment of commonly used active radiation protection dosimeters for individual and area workplace monitoring, *Journal of Radiation Research and Applied Sciences*, Vol. 19, Iss. 1, 2026.

[13] International Organization for Standardization (ISO), 2019. ISO 4037-1:2019—Radiological Protection—X and Gamma Reference Radiation for Calibrating Dosimeters and Dose-Rate Meters and for Determining their Response as a Function of Photon Energy—Part 1: Radiation Characteristics and Production Methods. ISO, Geneva.

[14] International Electrotechnical Commission (IEC), 2005. IEC 61267: Medical Diag-nostic X-Ray Equipment—Radiation Conditions for Use in the Determination of Characteristics. IEC, Geneva

[15] L. Pavelić, I. Lacković, G. Jazvac, A. M. Kožuljević, L. Glavak Pavelić, I. Prlić, On measurement standards and techniques in performance evaluation of a modern X-ray generator, *Radiation Physics and Chemistry*, Vol. 241, 2026.

[16] Spherical Chamber 1 Liter 32002, Spherical ionization chamber for radiation protection measurement, PTW, https://www.ptwdosimetry.com/en/products-metrology/spherical-chamber-1-liter-32002/

[17] FH 40 G Multi-Purpose Digital Survey Meter, Thermo Fisher Scientific, https://www.thermofisher.com/order/catalog/product/4254008

[18] Thermo FHZ 312A, High dose rate underwater probe for FH 40G, Thermo Fisher Scientific, https://documents.thermofisher.com/TFS-Assets/CAD/Specification-Sheets/54144TD-E.pdf

[19] SPIR-Ace Radionuclide Identification Device (RIID) with quantitative assessment capability, Mirion Technologies, https://www.mirion.com/products/technologies/defense-security-systems/security-search-systems/handheld-radioisotope-identification-devices/spir-ace-radionuclide-identification-device-riid-with-quantitative-assessment-capability

[20] Survey Meter OD-02, STEP Sensortechnik und Elektronik Pockau GmbH, https://www.step-sensor.de/english/radiation-mesurement/survey-meters/

[21] BeOSL Area Dosimeter, Mirion Technologies, https://www.mirion.com/products/medical/occupational-dosimetry/dosimetry-systems/modular-beosl-systems/osl-area-dosimeter

[22] J. F. Boudreau, E. S. Swanson, Interpolation and extrapolation, *Applied Computational Physics,* Oxford University Press, 2017.

[23] JCGM 100:2008(E), Evaluation of measurement data — Guide to the expression of uncertainty in measurement (GUM) with minor corrections, 1995.

[24] W. Lechner, H. Palmans, Uncertainty estimation for dosimetry in radiation oncology, *Physics and Imaging in Radiation Oncology*, Vol. 34, 2025.

[25] Python GUM Tree Calculator package, https://gtc.readthedocs.io/en/stable/index.html